blood®
Regular Article

TRANSFUSION MEDICINE

Increased erythrophagocytosis induces ferroptosis in red pulp macrophages in a mouse model of transfusion

Lyla A. Youssef,[1] Abdelhadi Rebbaa,[2] Sergey Pampou,[3] Stuart P. Weisberg,[2] Brent R. Stockwell,[4,5] Eldad A. Hod,[2] and Steven L. Spitalnik[2]

[1]Department of Microbiology and Immunology, [2]Department of Pathology and Cell Biology, [3]J. P. Sulzberger Columbia Genome Center, [4]Department of Biological Sciences, and [5]Department of Chemistry, Columbia University, New York, NY

KEY POINTS

- Transfusions of storage-damaged RBCs induce an RPM-dependent inflammatory response by splenic Ly6C^{hi} monocytes.
- Macrophages undergo ferroptosis following increased erythrophagocytosis and are replaced by circulating monocytes and local cell division.

Macrophages play important roles in recycling iron derived from the clearance of red blood cells (RBCs). They are also a critically important component of host defense, protecting against invading pathogens. However, the effects on macrophage biology of acutely ingesting large numbers of RBCs are not completely understood. To investigate this issue, we used a mouse model of RBC transfusion and clearance, which mimics the clinical setting. In this model, transfusions of refrigerator storage-damaged (ie, "old") RBCs led to increased erythrophagocytosis by splenic red pulp macrophages (RPMs). This robust erythrophagocytosis induced ferroptosis, an iron-dependent form of cell death, in RPMs. This was accompanied by increases in reactive oxygen species and lipid peroxidation in vivo, which were reduced by treatment in vitro with ferrostatin-1, a ferroptosis inhibitor. Old RBC transfusions also induced RPM-dependent chemokine expression by splenic Ly6C^{hi} monocytes, which signaled Ly6C^{hi} monocyte migration from bone marrow to spleen, where these cells subsequently differentiated into RPMs. The combination of cell division among remaining splenic RPMs, along with the influx of bone marrow–derived Ly6C^{hi} monocytes, suggests that, following RPM depletion induced by robust erythrophagocytosis, there is a coordinated effort to restore homeostasis of the RPM population by local self-maintenance and contributions from circulating monocytes. In conclusion, these findings may be clinically relevant to pathological conditions that can arise as a result of increased erythrophagocytosis, such as transfusion-related immunomodulation and impaired host immunity. (*Blood*. 2018;131(23):2581-2593)

Introduction

Erythrophagocytosis of senescent red blood cells (RBCs) is important for the physiological iron recycling necessary for normal erythropoiesis. In humans, RBCs have a lifespan of ~120 days before being recycled by hepatic and splenic phagocytes. However, multiple disorders lead to a shortened RBC lifespan and increased or pathologic erythrophagocytosis, including malaria,[1] immunoglobulin G (IgG)–mediated hemolytic transfusion reactions,[2] warm-type autoimmune hemolytic anemia,[3] and acute hemolytic crises in sickle cell disease or glucose-6-phosphate dehydrogenase deficiency.[4] RBC transfusions can also induce a rapid increase in erythrophagocytosis due to acute clearance of refrigerator storage-damaged RBCs.[5] Given the critically important role that phagocytes play in host defense, if acutely increased erythrophagocytosis harmed phagocyte function, this could predispose the host to transfusion-mediated immunomodulation (TRIM) and harmful infectious consequences.

Following phagocytosis of "effete" RBCs, by any recognition mechanism, their hemoglobin is degraded in the lysosomal system and a proportion of the resulting inorganic iron is released from the phagocyte into plasma by ferroportin; this iron is subsequently transported through the circulation by transferrin. However, if "free" iron is present in plasma or cytosol, it is highly reactive and can participate in multiple redox reactions. For example, Fe^{2+} reacts with peroxides to produce hydroxyl and lipid alkoxy radicals through the Fenton reaction, thereby producing multiple reactive oxygen species (ROS) and lipid peroxidation products.[6] Thus, to minimize its adverse effects, iron is typically bound by an array of chaperones. For example, cytosolic ferritin assists in storing iron intracellularly, converting reactive Fe^{2+} into oxidized Fe^{3+}.[7,8]

Nonetheless, in certain clinical situations (see previous paragraphs), macrophages are subjected to an acute and substantial increase in erythrophagocytosis. Following increases in erythrophagocytosis and intracellular heme, macrophage cell loss is observed.[9,10] However, the causes of the effects of this robust erythrophagocytosis on macrophages are still not completely clear, but may result from the large iron load that is abruptly delivered to these cells. In this context, we hypothesized that increased erythrophagocytosis would induce macrophage

ferroptosis, an iron-dependent form of nonapoptotic cell death originally identified in cancer cells,[11] but not yet studied following macrophage erythrophagocytosis. Ferroptosis is characterized by increased ROS and lipid peroxidation due to metabolic dysfunction.[11,12] If pathologic erythrophagocytosis did indeed induce phagocyte cell death, this could negatively affect host immunity, particularly with regard to infectious pathogens.

To investigate these issues, we used a mouse model of RBC storage and transfusion that closely mimics the human setting, including achieving similar posttransfusion RBC recovery and lifespan.[13] RBC transfusions are the most common therapeutic intervention in hospitalized patients, with ~12 million RBC units administered annually in the United States[14] for multiple indications (eg, trauma, surgery, and cancer). Despite clear clinical benefits, RBC transfusions are often associated with adverse effects, including an increased risk of bacterial infection in patients and animal models.[15-21] In addition, in animal models, transfusions of refrigerator storage-damaged RBCs acutely increase circulating levels of multiple cytokines.[5,22]

In the United States, human donor RBCs are refrigerator-stored for up to 42 days, during which they undergo multiple structural and metabolic alterations, collectively known as "the storage lesion."[23-26] As a result, a substantial proportion of storage-damaged RBCs (ie, up to 25%) are rapidly cleared from the circulation after transfusion, primarily by hepatic and splenic phagocytes.

In our mouse model, transfusions of refrigerator storage-damaged (ie, "old") RBCs enhanced erythrophagocytosis by splenic red pulp macrophages (RPMs). This robust erythrophagocytosis induced RPM ferroptosis, accompanied by increases in ROS and lipid peroxidation in vivo, all of which were reduced in vitro by ferrostatin-1, a ferroptosis inhibitor. Old RBC transfusions also induced RPM-dependent chemokine expression by splenic Ly6C^{hi} monocytes, which signaled Ly6C^{hi} monocyte migration from the bone marrow to the spleen, where these cells subsequently differentiated into RPMs. The combination of cell division among remaining splenic RPMs, along with the influx of bone marrow–derived Ly6C^{hi} monocytes, suggests that, following RPM depletion induced by robust erythrophagocytosis, there is a coordinated effort to restore homeostasis of the RPM population by both local self-maintenance and contributions from circulating monocytes. Nonetheless, before homeostasis is achieved, this RPM depletion could predispose the host to adverse consequences (eg, infection) resulting from defective immune function.

Materials and methods

Mice

Wild-type C57BL/6, *CCR2*$^{-/-}$ (on a B6.129S4 background), and C57BL/6-Tg (UBC-GFP [green fluorescent protein]) mice were purchased from The Jackson Laboratory. MaFIA (Csfr1-EGFP) mice (on a C57BL/6 background) were a generous gift from Anthony Ferrante (Columbia University Medical Center). *Spic*$^{-/-}$ mice (on a 129/SvEv background) were a generous gift from Kenneth Murphy (School of Medicine, Washington University in St. Louis). CCL2-GFP reporter mice (on a C57BL/6 background) were a generous gift from Eric Pamer (Memorial Sloan Kettering Cancer Center). Mice were used at 6 to 12 weeks of age. All procedures were approved by the institutional animal care and use committee at Columbia University.

RBC collection and transfusions

Wild-type C57BL/6 mice or UBC-GFP mice were bled aseptically via cardiac puncture and pooled whole blood was placed in CPDA-1 solution that was obtained from di-(2-ethylhexyl) phthalate–plasticized polyvinyl chloride human primary collection packs (Baxter, Deerfield, IL) to a final concentration of 15% CPDA-1. Whole blood was then leukoreduced using a neonatal high-efficiency leukocyte reduction filter (Purecell Neo; Pall Corporation, Port Washington, NY). Leukoreduced blood was centrifuged at 1000*g* for 10 minutes to pack the RBCs and a portion of the plasma-containing CPDA-1 supernatant was removed to yield a ~75% hematocrit. Leukoreduced, packed RBCs were either used "fresh" (ie, stored for <24 hours at 4°C) or "old" (ie, stored for 12-14 days at 4°C).

Isoflurane-anesthetized mice were transfused with either 200 or 350 μL of packed RBCs through the retro-orbital plexus. At defined times posttransfusion, mice were anesthetized with isoflurane, sacrificed, and the spleen, bone marrow, and blood were collected.

Cell isolation, flow cytometric analysis, and sorting

Splenocytes were isolated after homogenizing spleens using a test tube with a cell-strainer cap. Bone marrow was harvested by flushing the femur with a 25G 5/8" needle (Becton Dickinson [BD], Franklin Lakes, NJ) using phosphate-buffered saline (PBS) containing 1% fetal bovine serum (FBS) (HyClone; GE Healthcare, Chicago, IL). Following RBC lysis, remaining cells were blocked using rat anti-mouse CD16/CD32 (BD Pharmingen, San Jose, CA) in PBS containing 1% FBS. Antibodies that were used recognized the following antigens: CD11b (M1/70; eBioscience, San Diego, CA), CD11c (N418), F4/80 (BM8), Ly6C (HK1.4; eBioscience), Ly6G (1A8), T-cell receptor β (H57-597), CD19 (6D5), CD3e (145-2C11; eBioscience), B220 (RA3-6B2), CD45 (30-F11), major histocompatibility complex II (MHCII; M5/114.152), CD115 (AFS98), and VCAM-1 (CD106, 429); the clonal designations are provided and all antibodies were purchased from BioLegend (San Diego, CA), unless otherwise indicated. Annexin V was purchased from BD Pharmingen. Cell suspensions were analyzed using LSRII, LSRFortessa, or C6 Accuri cytometers (BD). Fluorescence-activated cell sorting (FACS) was performed using the Influx instrument (BD). All flow cytometry data were analyzed with FlowJo software (BD, Ashland, OR) or FCS Express software (De Novo Software, Los Angeles, CA).

Quantitative reverse-transcriptase PCR

Designated splenic macrophage and monocyte populations were sorted into TRIzol (Invitrogen, Carlsbad, CA) for RNA extraction followed by processing with SuperScript VILO (Invitrogen) for complementary DNA synthesis. Quantitative polymerase chain reaction (PCR) was then performed using QIAGEN (Germantown, MD) RT2 SYBR Green master mix and normalized to the housekeeping gene *GAPDH*. The primer sequences used were:

CCL2 forward primer sequence: CCTGGATCGGAACCAAA TGAGATCAG

CCL2 reverse primer sequence: AGTGCTTGAGGTGGTTG TGGAA

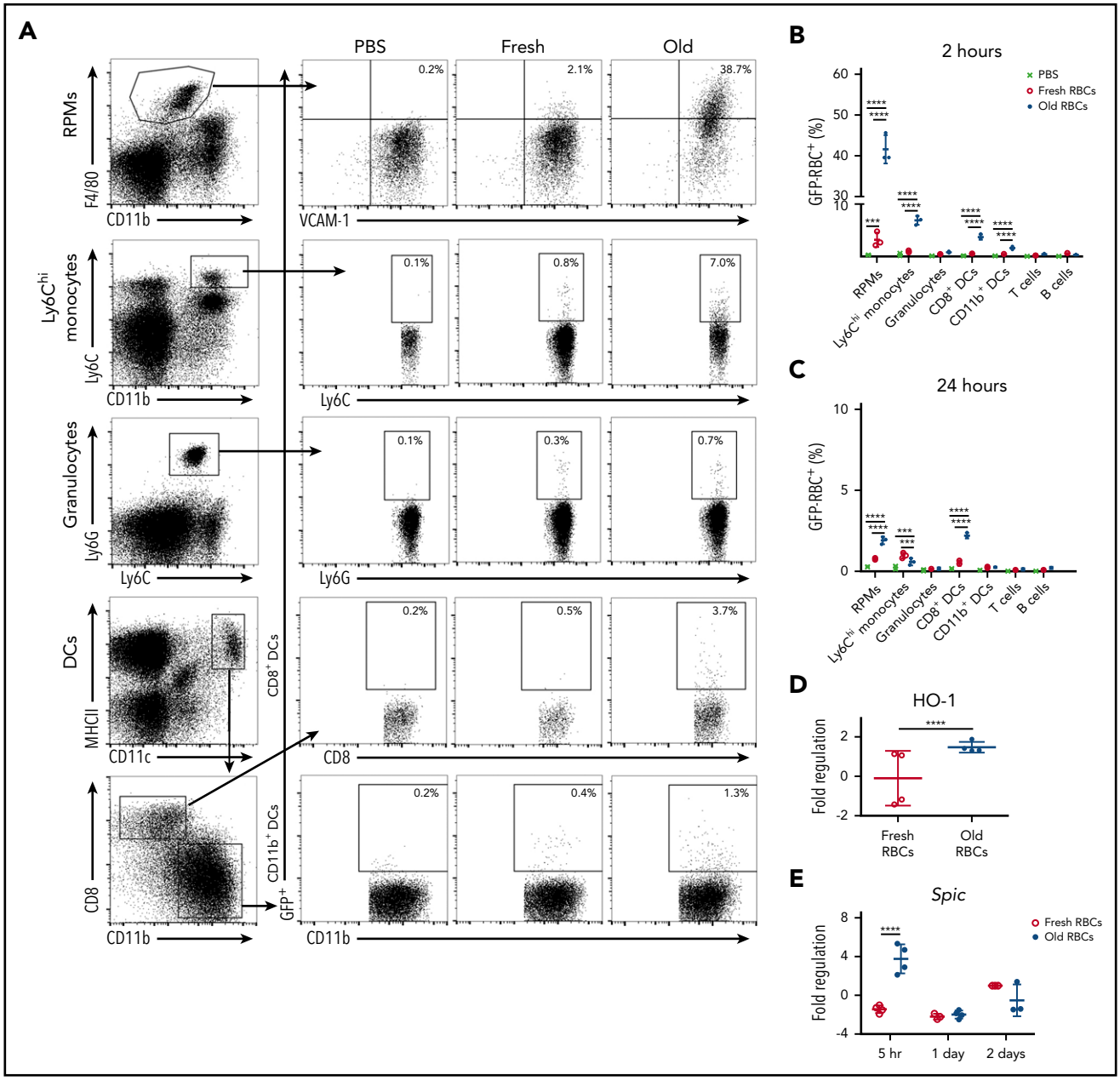

Figure 1. RPMs are the predominant splenic population responsible for phagocytosis of old RBCs, with Ly6C^{hi} monocytes also contributing to RBC clearance. Wild-type C57BL/6 mice were transfused with 200 μL of PBS, fresh GFP$^+$ RBCs, or old GFP$^+$ RBCs. Mice were then sacrificed at 2 or 24 hours posttransfusion. (A) Representative dot plots show the gating strategy for RPMs (F4/80^{hi}, VCAM-1$^+$, CD11b^{lo}), Ly6C^{hi} monocytes (Ly6C^{hi}, CD11b^{hi}), granulocytes (Ly6G$^+$, Ly6C$^+$, CD11b$^+$), CD8$^+$ DCs (CD8$^+$, CD11b$^-$, MHCII^{hi}, CD11c^{hi}), and CD11b$^+$ DCs (CD8$^-$, CD11b$^+$, MHCII^{hi}, CD11c^{hi}) at 2 hours posttransfusion. These cells were obtained from the spleen at 2 hours posttransfusion. Percentages of GFP$^+$ cells are depicted; these represent nucleated cells that have phagocytosed GFP-expressing fresh or old transfused RBCs. (B) Frequency of GFP$^+$ RBC phagocytosis at 2 and (C) 24 hours posttransfusion; by 24 hours posttransfusion, the levels of phagocytosis were dramatically reduced compared with the 2-hour time point and the previously ingested GFP$^+$ RBCs were degraded. (D) *Hmox-1* (ie, HO-1) expression by RPMs 5 hours posttransfusion. (E) *Spic* expression by Ly6C^{hi} monocytes 5 hours posttransfusion. Data representative of 4 experiments with at least 3 mice per group; *$P < .05$; ***$P < .001$; ****$P < .0001$; ANOVA with Tukey or Sidak multiple comparison test.

CCL7 forward primer sequence: GGTGTCCCTGGGAAGCTG TTAT

CCL7 reverse primer sequence: TATAGCCTCCTCGACCCAC TTCT

GAPDH forward primer sequence: ATGACTCCACTCACGGCA AATTC

GAPDH reverse primer sequence: ACACCAGTAGACTCCACGA CATAC.

Adoptive transfer

Bone marrow was collected from UBC-GFP mice and RBCs were lysed. The remaining cells were incubated with rat anti-mouse CD16/CD32 (BD Pharmingen) and then with biotinylated antibodies recognizing the following antigens for negative selection of monocytes: CD11c (N418), CD3e (145-2C11; eBioscience), Ly6G (1A8), B220 (RA3-6B2), F4/80 (BM8; eBioscience), NK1.1 (PK136), CD49b (DX5), and CD34 (RAM34; eBioscience); all

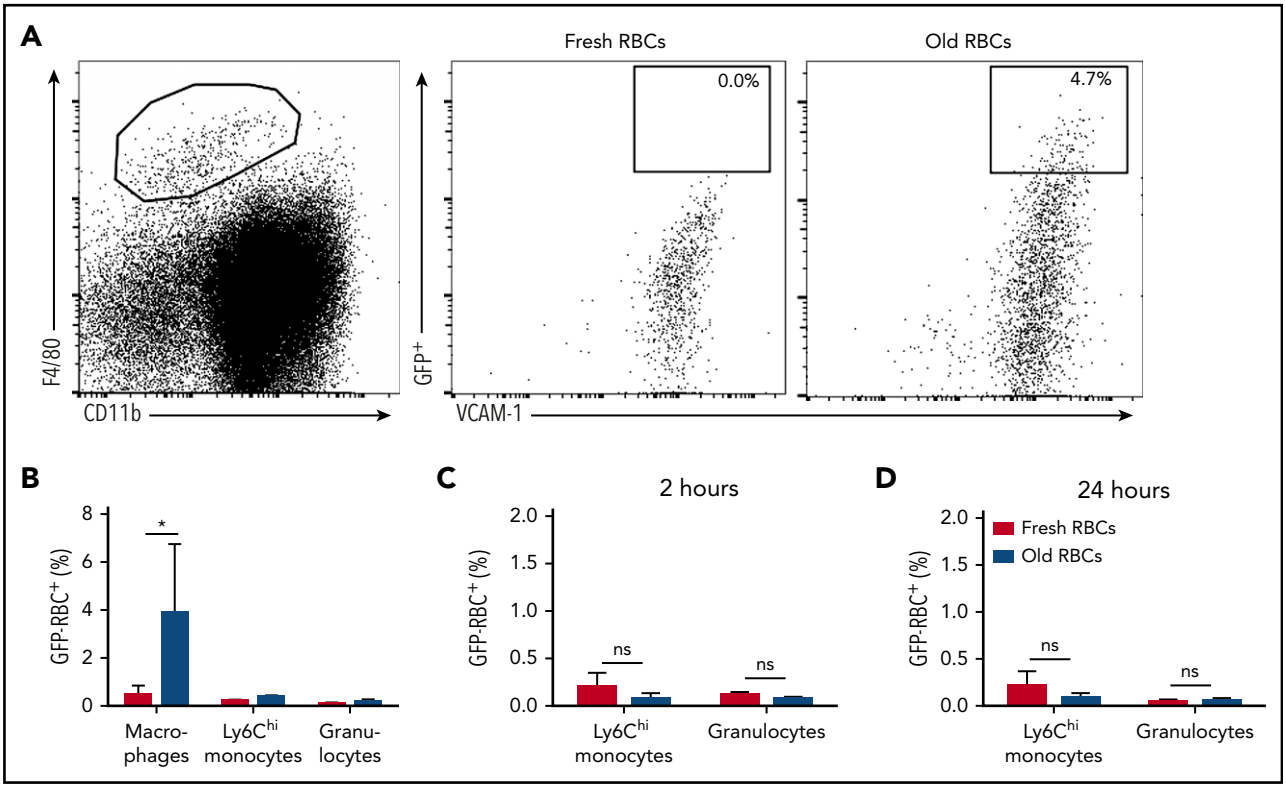

Figure 2. VCAM-1$^+$, F4/80^{hi} bone marrow macrophages ingest transfused old RBCs. (A) Gating strategy for identifying bone marrow macrophages (VCAM-1$^+$, F4/80^{hi}, CD11b^{lo}) that phagocytose transfused RBCs (GFP$^+$). (B) Frequency of phagocytosis of old RBCs at 2 hours posttransfusion by bone marrow macrophages, Ly6C^{hi} monocytes and granulocytes; although macrophages ingest some transfused RBCs, no such phagocytosis is seen with Ly6C^{hi} monocytes or granulocytes. (C-D) Frequency of ingested GFP$^+$ RBCs at 2 and 24 hours posttransfusion in circulating Ly6C^{hi} monocytes and granulocytes. Data representative of 3 experiments with at least 3 mice per group. *$P < .05$; ANOVA with Tukey or Sidak multiple comparison test. ns, not significant.

antibodies were purchased from Biolegend, unless otherwise indicated. Monocytes (1×10^6) were infused into anesthetized mice through the retro-orbital plexus followed by infusions of PBS or transfusions of old RBCs.

Lipid peroxidation and ROS studies

To measure lipid peroxidation, splenocytes, J774A.1 cells (J774; purchased from ATCC, Manassas, VA), or bone marrow–derived macrophages (BMDMs) were incubated with C11-Bodipy 581/591 (Molecular Probes, Invitrogen) following either transfusion in vivo or incubation with RBCs in vitro at 37°C. Isolated cells were washed twice with PBS containing 1% FBS and then either stained for surface markers or immediately analyzed by flow cytometry, where increases in lipid peroxidation were determined by increases in intensity in the FL-1 channel. To measure ROS production, splenocytes, J774 cells, or BMDMs were incubated with 2′,7′-dichlorodihydrofluorescein diacetate (H2-DCFDA; Molecular Probes, Invitrogen) for 30 minutes at 37°C following transfusion or incubation with RBCs. Cells were washed twice and then either stained for surface markers or immediately analyzed by flow cytometry. The H2-DCFDA assay is useful for measuring ROS in cells despite detecting changes in other constituents in addition to increases in hydrogen peroxide.[27]

In vitro erythrophagocytosis assay

J774 cells were cultured in Dulbecco minimal essential medium supplemented with 10% FBS, 2 mM L-glutamine, penicillin (50 U/mL), and streptomycin (50 μg/mL). To prepare primary BMDMs, mononuclear cells obtained from mouse femurs were cultured in 20 ng/mL macrophage colony-stimulating factor (PeproTech, Rocky Hill, NJ) in Iscove modified Dulbecco medium supplemented with 10% FBS, 2 mM L-glutamine, penicillin (50 U/mL), streptomycin (50 μg/mL), and 20 μg/mL gentamycin (Gibco/Life Technologies, Carlsbad, CA) for 7 to 11 days. J774 cells or BMDMs were plated 24 hours prior to the day of the experiment. On the day of the experiment, fresh RBCs were fluorescently labeled with CellTrace Far Red (Invitrogen) and then incubated with IgG anti-RBC antibody at 0.5 mg/mL (rabbit anti-mouse, polyclonal; Rockland Immunochemicals, Limerick, PA) to generate opsonized RBCs. Adherent phagocytes were then incubated with PBS, nonopsonized RBCs, or opsonized RBCs for 2 hours at 37°C. Following incubation, noningested RBCs were lysed and adherent cells were removed by scraping or by incubation with Accutase (eBioscience) at 37°C. Cells were then analyzed by flow cytometry.

High-throughput microscopy assay

Black polystyrene 96-well plates (Greiner, Monroe, NC) were used to culture BMDMs 72 hours prior to the experiment. On the day of the experiment, adherent cells were incubated with PBS, nonopsonized RBCs, or IgG-opsonized RBCs in combination with defined concentrations of ferrostatin-1 (Fer-1; Sigma-Aldrich, St. Louis, MO) or dimethyl sulfoxide (vehicle control) for 6 hours. Noningested RBCs were lysed and adherent cells stained with 4′,6-diamidino-2-phenylindole (Invitrogen) to

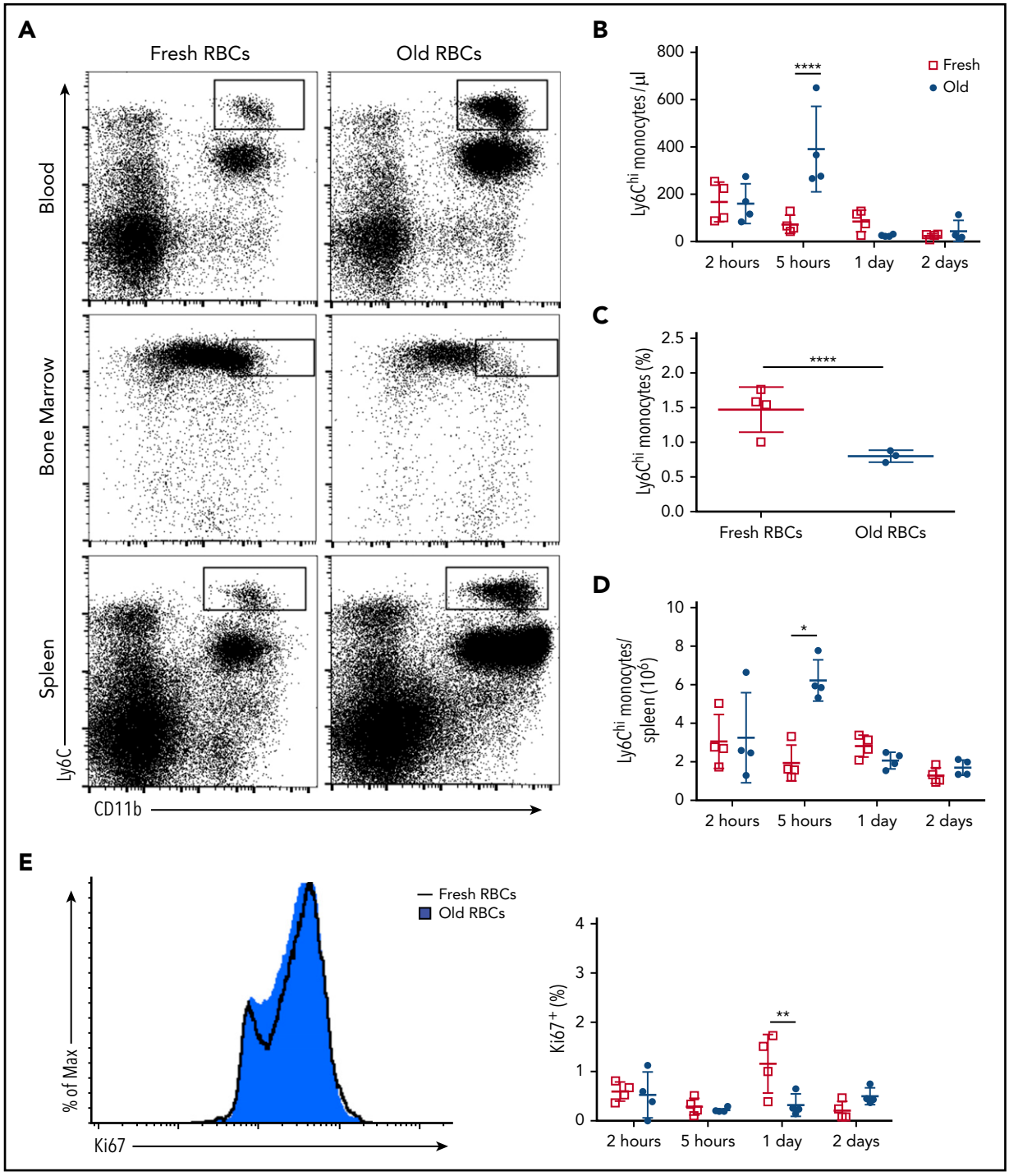

Figure 3. Ly6C^{hi} monocytes emigrate from the bone marrow and home to the spleen after transfusion of old RBCs. Wild-type C57BL/6 mice were transfused with 350 μL of fresh or old RBCs and sacrificed at defined time points. (A) Flow plots depict increases in Ly6C^{hi} monocytes in the blood and spleen and a decrease in the bone marrow at 5 hours posttransfusion. (B) Quantification of circulating Ly6C^{hi} monocytes at defined time points demonstrating increased levels at 5 hours posttransfusion. (C) Quantification of bone marrow Ly6C^{hi} monocytes demonstrating decreased levels at 5 hours posttransfusion. (D) Splenic Ly6C^{hi} monocyte levels increase substantially at 5 hours posttransfusion. (E) Histogram of Ki67 staining of splenic Ly6C^{hi} monocytes at 5 hours posttransfusion. Data representative of 3 experiments with at least 3 mice per group. *$P < .05$; **$P < .01$; ****$P < .0001$; ANOVA followed by Tukey posttest.

determine cell viability and total cell number, respectively. Plates were imaged on the IN Cell Analyzer 2000 (GE Healthcare) and analyzed using IN Cell Investigator software (GE Healthcare).

Statistical analysis

Values on graphs are depicted as mean ± standard deviation. Calculations for statistical differences between various groups were carried out by the analysis of variance (ANOVA) technique and the Sidak, Tukey, or Dunnett posttest to correct for multiple comparisons, which are indicated in the figure legends. Otherwise, a 2-tailed unpaired Student *t* test was used. Statistical significance is expressed as follows: *$P < .05$; **$P < .01$; ***$P < .001$; ****$P < .0001$. GraphPad (La Jolla, CA) PRISM software version 6.0 was used for all statistical analyses.

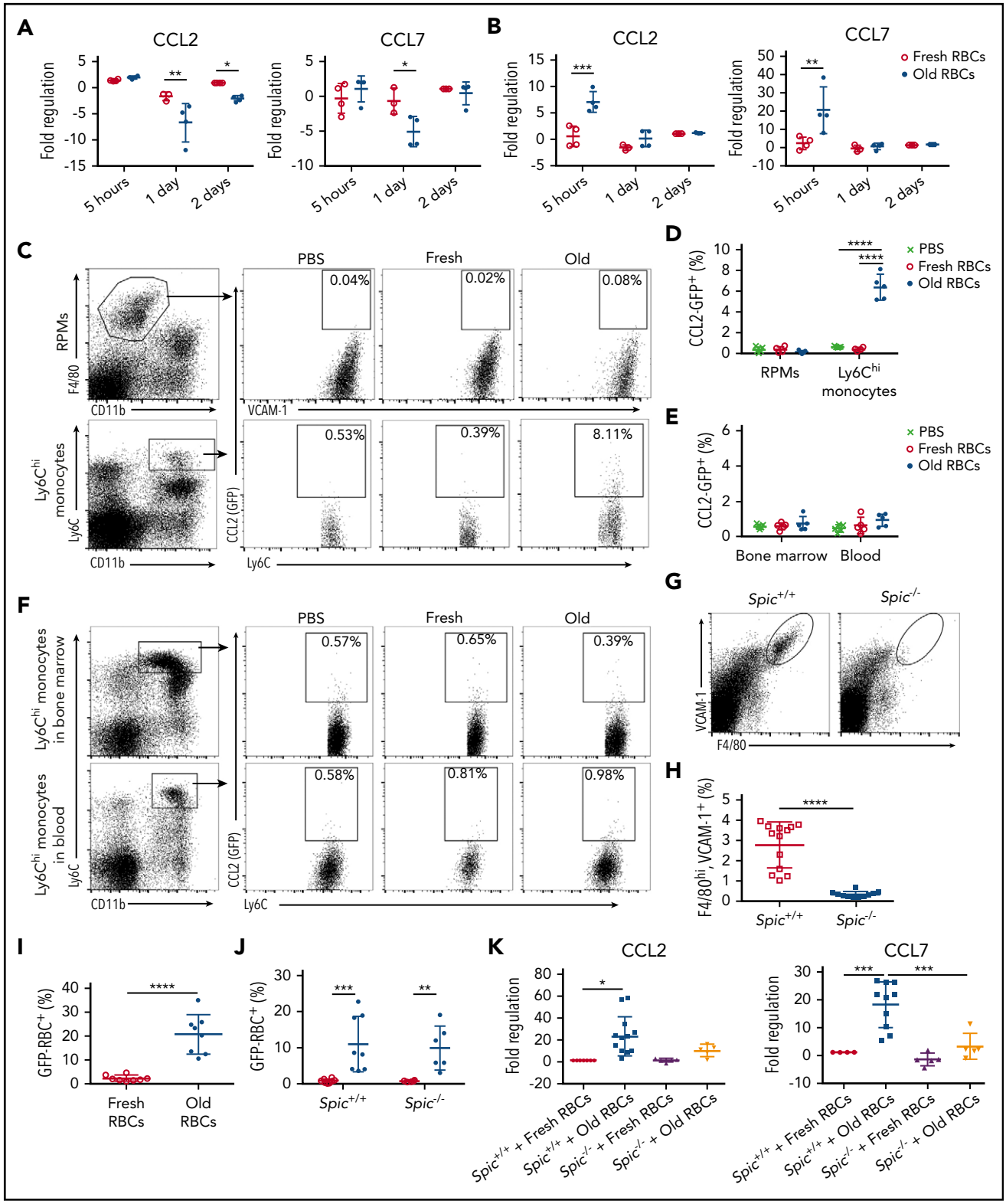

Figure 4. CCL2 and CCL7 mRNA expression by splenic Ly6C^{hi} monocytes following enhanced erythrophagocytosis requires the presence of RPMs. At defined time points after transfusing wild-type recipients with 350 μL of fresh or old RBCs, splenocytes were isolated by FACS, and CCL2 and CCL7 mRNA expression was measured by qPCR in (A) RPMs and (B) Ly6C^{hi} monocytes; these data show that, after old RBC transfusions, expression of these chemokines did not change, or even decreased, in RPMs, whereas they both increased substantially in Ly6C^{hi} monocytes at 5 hours posttransfusion. CCL2-GFP reporter mice were transfused with 200 μL of PBS, fresh GFP$^+$ RBCs, or old GFP$^+$ RBCs, and then sacrificed at 2 hours posttransfusion. (C) Gating strategy for splenic RPMs and Ly6C^{hi} monocytes along with representative dot plots showing induced *CCL2* promoter–dependent GFP expression; the percentages of cells expressing GFP are provided. (D) Frequency of GFP expression, demonstrating upregulation by Ly6C^{hi} monocytes, but not by RPMs. (E) Frequency of CCL2 expression by RPMs and Ly6C^{hi} monocytes showing no statistically significant changes posttransfusion. (F) Gating strategy for Ly6C^{hi} monocytes in the blood and bone marrow, along with representative dot plots showing *CCL2* promoter–dependent GFP expression; the percentages of cells expressing GFP are provided. To determine the dependence of Ly6C^{hi} monocyte *CCL2* and *CCL7* mRNA expression on the presence of RPMs, *Spic*$^{-/-}$ mice were used for

Results

RPMs are the predominant splenic population that clears transfused old RBCs

Packed, leukoreduced RBCs were prepared from UBC-GFP donor mice and used "fresh" or after 12 to 14 days of storage (ie, "old") under conditions that mimic those in clinical blood banks. By 2 hours after transfusing 200 μL of fresh or old packed RBCs into recipient mice (roughly equivalent to a 1-unit transfusion in humans), a significant proportion of splenic RPMs (VCAM-1^{+}, F4/80^{hi}, CD11b^{lo}) had already ingested old, but not fresh, RBCs (38.2% and 2.1%, respectively) (Figure 1A-B). This clearance of old transfused RBCs occurred rapidly, and erythrophagocytosis dramatically decreased by 24 hours posttransfusion (Figure 1C). The increase in erythrophagocytosis also coincided with an increase in *Hmox1* messenger RNA (mRNA) content (Figure 1D); its protein translation product, heme oxgenase-1 (HO-1), is required to metabolize and detoxify heme. Splenic Ly6C^{hi} monocytes (Ly6C^{hi}, CD11b^{+}, CD115^{+}, Ly6G^{-}) also cleared old RBCs, however, at a lower level than RPMs (7.02%; Figure 1A-C) and exhibited increased *Spic* mRNA expression, a heme responsive gene,[28] by 5 hours posttransfusion (Figure 1E). In contrast, splenic granulocytes, as well as those in the bone marrow and the circulation, which are typically highly active phagocytes, particularly for pathogenic bacteria and IgG-coated RBCs,[29] exhibited very little erythrophagocytosis in this setting (Figures 1A-C and 2B-D). CD8^{+} and CD11b^{+} dendritic cells (DCs) also displayed low levels of erythrophagocytosis (Figure 1A-C), both at 2 and 24 hours posttransfusion. However, splenic lymphocytes did not ingest old RBCs (Figure 1B-C). Nonetheless, a proportion of bone marrow macrophages (VCAM-1^{+}, F4/80^{hi}, CD11b^{lo}) also cleared old transfused RBCs (3.88%; Figure 2A-B). However, Ly6C^{hi} monocytes in the blood and bone marrow did not selectively clear old RBCs (Figure 2B-D). Taken together, these results highlight the major role that the mononuclear phagocyte system, particularly splenic RPMs, plays in clearing old transfused RBCs.

Old RBC transfusions induce Ly6C^{hi} inflammatory monocyte trafficking to the spleen

Ly6C^{hi} monocytes can emigrate from the bone marrow in response to specific chemokines, including CCL2 and CCL7, which can engage their cell surface receptor: CCR2.[30-32] Old, but not fresh, RBC transfusions induced a dramatic increase in circulating Ly6C^{hi} monocytes in recipients, which peaked at 5 hours posttransfusion and returned to steady-state levels by 24 hours posttransfusion (Figure 3A-B). This increase in Ly6C^{hi} monocytes coincided with a concomitant decrease in the number of these cells in the bone marrow (Figure 3A,C). The number of Ly6C^{hi} monocytes in the spleen also increased at 5 hours posttransfusion and returned to steady-state levels by 24 hours posttransfusion (Figure 3A,D). Based on Ki67 staining, splenic Ly6C^{hi} monocytes did not actively proliferate posttransfusion (Figure 3E). These findings suggest that the posttransfusion increase in splenic Ly6C^{hi} monocytes resulted from migration of these cells from the bone marrow, not from proliferation in situ of preexisting splenic Ly6C^{hi} monocytes.

Splenic Ly6C^{hi} monocytes upregulate *CCL2* and *CCL7* mRNA expression in an RPM-dependent fashion following enhanced erythrophagocytosis

To understand the influx of Ly6C^{hi} monocytes into the circulation, we examined whether a splenic cell population was a source of chemokines that might signal this migration. To this end, in recipients of old RBC transfusions, RPMs did not upregulate expression of *CCL2* or *CCL7* mRNA, and actually downregulated their expression by 1 day posttransfusion (Figure 4A). This was confirmed using CCL2-GFP reporter mice (Figure 4C-D). In contrast, by 5 hours after transfusion of old RBCs, Ly6C^{hi} monocytes dramatically increased their expression of *CCL7* and *CCL2* mRNA (20.55-fold and 7.00-fold, respectively), before returning to steady-state levels (Figure 4B-D). This was surprising because a relatively low percentage of Ly6C^{hi} monocytes phagocytose old RBCs, as compared with RPMs (Figure 1A-B). Using CCL2-reporter mice, there were no increases in *CCL2* expression in Ly6C^{hi} monocytes in blood or bone marrow, further highlighting an important role for neighboring RPMs in this phenomenon (Figure 4E-F).

Given the robust erythrophagocytosis by RPMs, we sought to determine whether expression of *CCL2* and *CCL7* mRNA by Ly6C^{hi} monocytes required RBC clearance by RPMs. To address this, we used *Spic*$^{-/-}$ mice, which lack Spi-C, a transcription factor that selectively controls RPM development,[33] and, therefore, lack RPMs (Figure 4G-H). *Spic*$^{+/+}$ and *Spic*$^{-/-}$ mice were transfused with fresh or old RBCs, and splenic Ly6C^{hi} monocytes were isolated by FACS at 5 hours posttransfusion. RPMs in *Spic*$^{+/+}$ mice effectively ingested old RBCs (Figure 4I). No difference in erythrophagocytosis by Ly6C^{hi} monocytes was observed in the absence of RPMs, indicating that RPMs are not required for erythrophagocytosis by these monocytes (Figure 4J). However, in the absence of RPMs, Ly6C^{hi} monocytes exhibited reduced *CCL2* and *CCL7* mRNA expression following old RBC transfusions (Figure 4K). This indicates that *CCL7* and *CCL2* mRNA expression by Ly6C^{hi} monocytes depends upon erythrophagocytosis by RPMs, suggesting that an "upstream mediator" produced by RPMs may induce expression of these chemokines in splenic Ly6C^{hi} monocytes.

Enhanced erythrophagocytosis induces increases in ROS, lipid peroxidation, and cell death in RPMs

RPM cell numbers substantially decreased by 2 hours after old, as compared with fresh, RBC transfusions and did not return to steady-state levels until 2 days posttransfusion (Figure 5A). This dramatic decrease in RPM cell numbers could be due to an artifact; that is, it may result from a phagocytosis-induced decrease in expression of the cell surface markers used to identify this population. To clarify this dilemma, we used MaFIA mice, which express enhanced green fluorescent protein (EGFP) under the control of the *Csfr1* promoter.[34] Using a specific strategy

Figure 4 (continued) the experiments in panels G-K. (G-H) RPMs (VCAM-1^{hi}, F4/80^{hi}) are absent in *Spic*$^{-/-}$ mice, as compared with *Spic*$^{+/+}$ controls. (I) The proportion of RPMs in *Spic*$^{+/+}$ recipient mice that ingested old GFP^{+} RBCs. (J) The proportions of Ly6C^{hi} monocytes in *Spic*$^{+/+}$ and *Spic*$^{-/-}$ mice that ingested old GFP^{+} RBCs. (K) Fold regulation of *CCL2* and *CCL7* mRNA expression, as measured by qPCR, in splenic Ly6C^{hi} monocytes from *Spic*$^{+/+}$ and *Spic*$^{-/-}$ mice. *$P < .05$; **$P < .01$; ***$P < .001$; ****$P < .0001$; ANOVA with Sidak or Tukey multiple comparisons test or unpaired *t* test. Data are representative of 3 independent experiments, except for *Spic*$^{+/+}$ and *Spic*$^{-/-}$ results, which were pooled for all experiments.

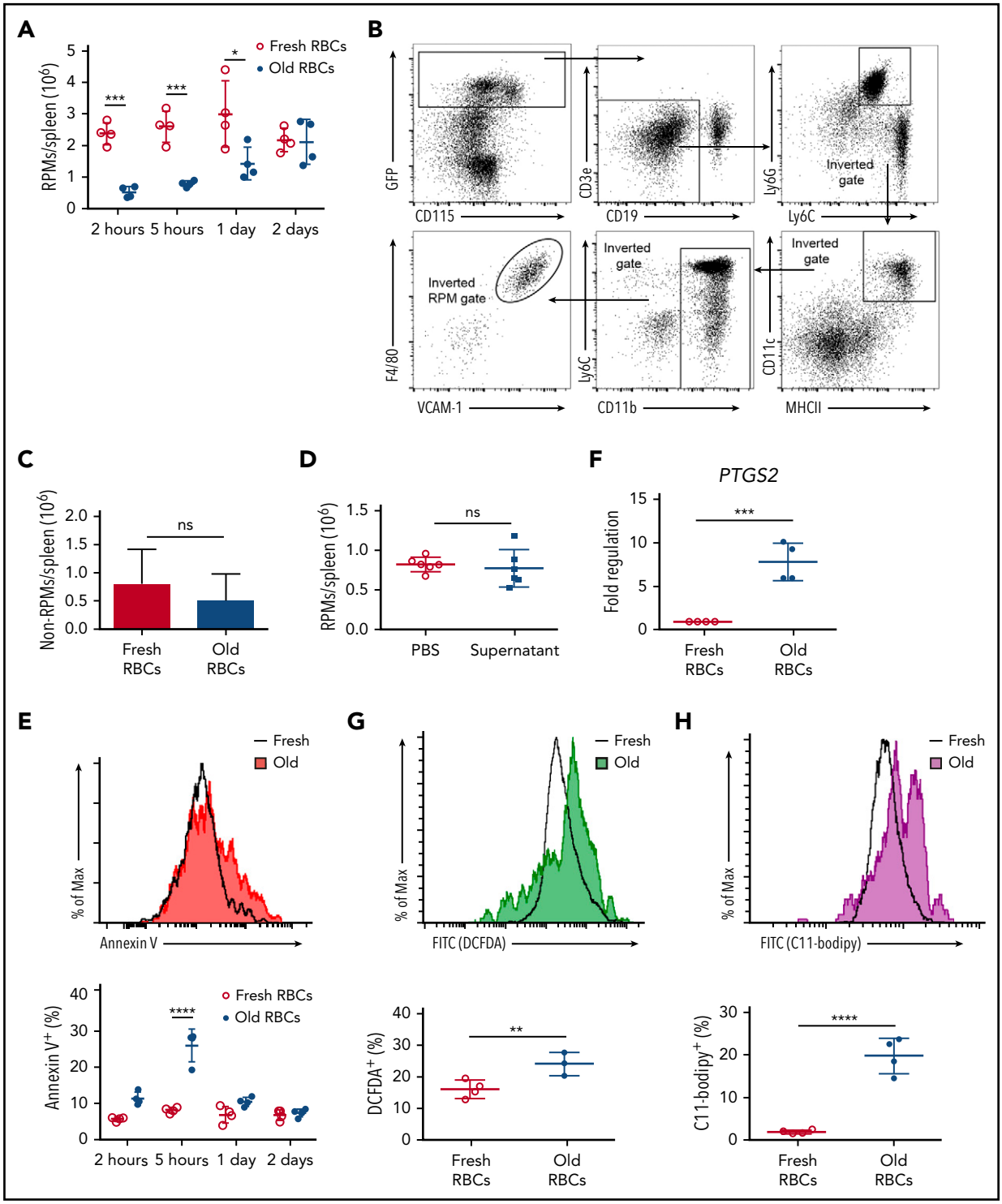

Figure 5. Transfusions of old RBCs induce oxidative stress, *PTGS2* expression, and cell death in RPMs. (A) Wild-type C57BL/6 mice were transfused with 350 μL of fresh or old RBCs and sacrificed at defined time points. Splenic RPM cell numbers were quantified posttransfusion. Old RBC transfusions induced a substantial decrease in RPMs by 2 hours posttransfusion, the levels of which returned to baseline 2 days later. (B) The gating strategy first selects for splenic nucleated non-RPM cells, which thereby selects for GFP$^+$ (Csfr1/CD115$^+$) cells; this is followed by gating out B cells, granulocytes, DCs, monocytes, and RPMs. The remaining cells were quantified to determine changes following transfusions of old, as compared with fresh, RBCs. (C) MaFIA mice were transfused with 350 μL of fresh or old RBCs and sacrificed 5 hours posttransfusion. Total non-RPM–nucleated cell numbers in the spleen were quantified, showing no differences. (D) Wild-type C57BL/6 mice were infused with PBS or supernatant from 350 μL of an old RBC blood bank and RPM cell number was quantified 5 hours posttransfusion. (E) Annexin V staining of RPMs following transfusion of old and fresh RBCs. (F) Upregulation of *PTGS2* mRNA expression in RPMs after old RBC transfusions. Increases in ROS production (G) and lipid peroxidation (H) in RPMs following transfusions of old RBCs. *$P < .05$; **$P < .01$; ***$P < .001$; ****$P < .0001$; ANOVA with the Sidak multiple comparisons test. *PTGS2* gene expression analysis was analyzed for significance using the unpaired Student *t* test. Data are representative of 3 independent experiments. FITC, fluorescein isothiocyanate.

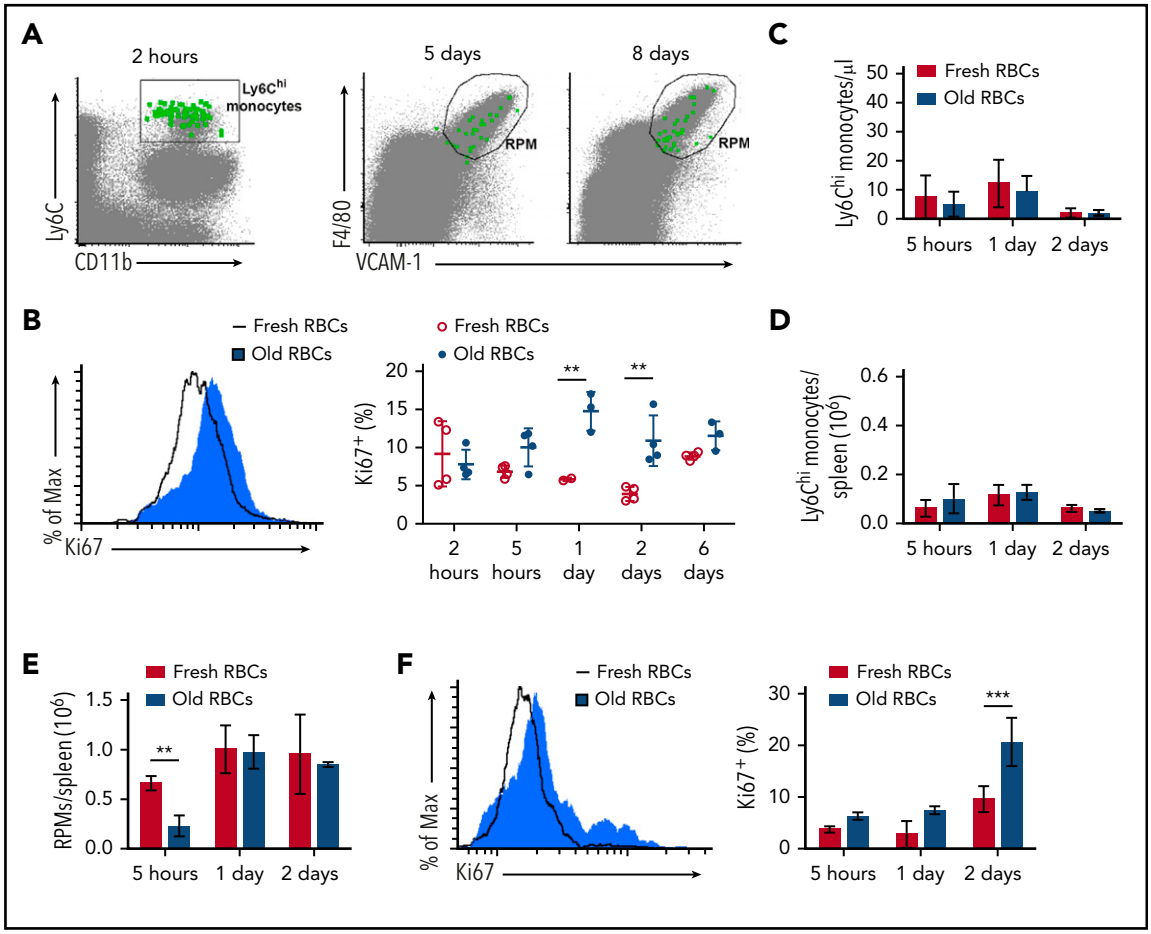

Figure 6. Splenic RPMs exhibit local self-maintenance following old RBC transfusion-induced cell death. (A) Bone marrow from UBC-GFP mice was harvested and enriched for Ly6C^{hi} monocytes by negative selection. GFP^{+}, Ly6C^{hi}, CD115^{+}, CD11b^{+} monocytes were then adoptively transferred to wild-type C57BL/6 recipients prior to transfusion of the latter with 350 μL of old RBCs. At 2 hours posttransfusion, GFP^{+} Ly6C^{hi} monocytes were observed in the spleen. By 5 and 8 days posttransfusion, GFP^{+} RPMs (F4/80^{hi}, VCAM-1^{hi}) were observed in the spleen. (B) Wild-type C57BL/6 mice were transfused with 350 μL of fresh or old RBCs and sacrificed at defined time points. Splenic RPMs were stained with Ki67, demonstrating increased proliferation at 1 to 2 days after old RBC transfusions, as compared with RPMs from mice that received fresh RBCs. Histogram (left) of Ki67 staining at 1 day posttransfusion. (C) Ly6C^{hi} monocyte cell numbers were quantified in the blood of *CCR2*$^{-/-}$ mice, demonstrating their absence. (D) Ly6C^{hi} monocyte cell numbers were quantified in the spleens of *CCR2*$^{-/-}$ mice, demonstrating their absence. (E) The splenic RPM population in *CCR2*$^{-/-}$ mice is reduced by 5 hours after transfusions of old RBCs, but restored by 2 days posttransfusion. (F) By Ki67 staining, RPMs in *CCR2*$^{-/-}$ mice proliferate following transfusion of old RBCs, relative to RPMs in mice that received fresh RBCs. Histogram (left) of Ki67 at 2 days posttransfusion. $^{**}P < .01$; $^{***}P < .001$; ANOVA with the Sidak posttest or unpaired Student *t* test. Data are representative of 3 independent experiments.

(Figure 5B), we gated for non-RPM, GFP-expressing cells to quantify the number of remaining cells. By this approach, when MaFIA mice were transfused with old, as compared with fresh, RBCs, there was no corresponding increase in non-RPMs to indicate that the RPMs were not being depleted, but instead had decreased surface expression of these identifying markers (Figure 5C); this confirms that RPM cell numbers do dramatically decrease following old RBC transfusions. However, no decrease in RPM cell numbers was observed in mice transfused with supernatant isolated from old stored RBCs, indicating that this cell loss is mediated by erythrophagocytosis, not by passive infusion of free hemoglobin, heme, or other compounds (Figure 5D). In addition, RPMs that ingested RBCs displayed increased Annexin V cell surface expression by 2 hours posttransfusion (11.27%), which peaked at 5 hours posttransfusion (25.96%), and returned to steady-state levels by 1 day posttransfusion (Figure 5E); thus, erythrophagocytosis induces phosphatidylserine exposure on RPMs, which is associated with various types of cell death. Furthermore, by quantitative PCR (qPCR) analysis, RPMs exhibited a 7.9-fold increased accumulation of prostaglandin-endoperoxide synthase 2 (*PTGS2*) mRNA, which encodes the cyclooxygenase-2 (COX-2) protein (Figure 5F); an increase in *PTGS2* mRNA levels is frequently induced in cells undergoing ferroptosis, and this process occurs downstream of lipid peroxidation.[12,35] In addition, by 2 hours after transfusion with old, as compared with fresh, RBCs, there were increases is DCF fluorescence, suggestive of ROS production (16.1%-24.1%; Figure 5G), and C11-Bodipy fluorescence, indicative of lipid peroxidation (2.0%-19.8%; Figure 5H); these phenomena are both observed concomitantly with ferroptosis, with lipid peroxidation being a particular hallmark of ferroptosis.

RPM population homeostasis is achieved following erythrophagocytosis-induced depletion by a combination of local RPM proliferation and differentiation of circulating monocytes

GFP^{+}Ly6C^{hi} monocytes that were adoptively transferred into wild-type recipients prior to transfusions with old RBCs migrated to the spleen by 2 hours posttransfusion (Figure 6A), further

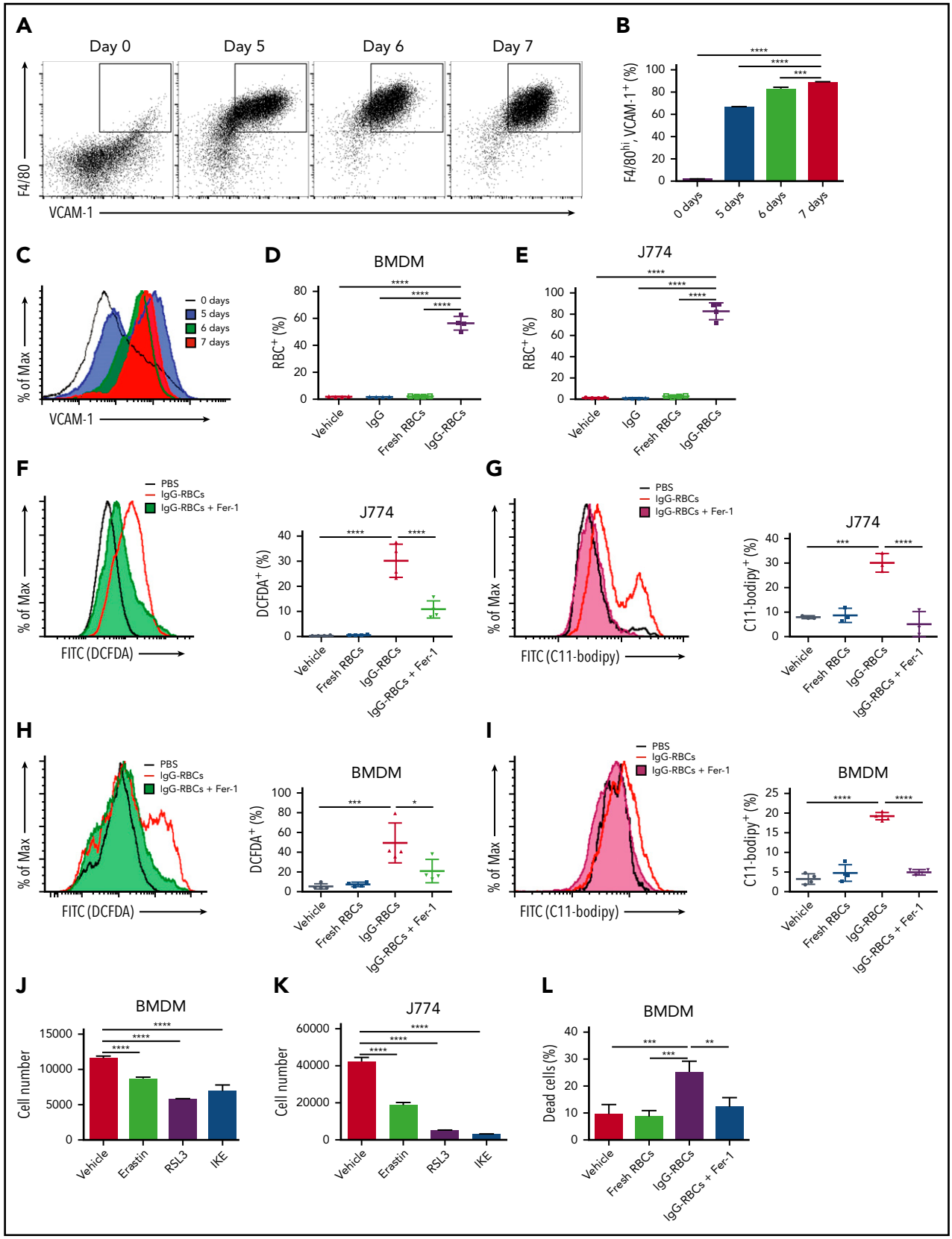

Figure 7. Enhanced erythrophagocytosis induces ferroptosis in macrophages in vitro. Bone marrow was harvested from wild-type C57BL/6 mice and cultured in the presence of macrophage colony-stimulating factor (20 ng/mL) for defined times to determine when the cell population uniformly expressed VCAM-1 and F4/80. (A) Representative dot plots (the percentages of double-positive cells are indicated), (B) frequency of VCAM-1$^+$, F4/80^{hi} macrophages, and (C) overall VCAM-1 expression are shown. BMDMs and J774 cells were plated 24 hours prior to the experiments and then incubated with PBS, fresh RBCs, or IgG-opsonized RBCs, which were labeled with CellTrace Far Red. The amount of erythrophagocytosis in (D) BMDMs and (E) J774 cells was quantified by flow cytometry. J774 cells (F-G) and BMDMs (H-I) were treated with vehicle control or

demonstrating that circulating Ly6C^{hi} monocytes traffic to the spleen in this model. By 5 days posttransfusion, GFP^{+} RPMs were observed in the spleen, indicating that the adoptively transferred monocytes had differentiated into RPMs (Figure 6A); thus, some monocytes that emigrate from the bone marrow to the spleen following transfusion of old RBCs eventually differentiate into RPMs to supplement the depleted population. These results support prior findings that RPMs are replaced by monocytes following heme-induced depletion.[28] However, RPMs are also capable of local self-maintenance by cell division.[36,37] Ki67 staining of RPMs at various time points following old RBC transfusion revealed that soon after transfusion-induced RPM cell loss, the remaining RPMs begin to proliferate, thereby helping to replace the diminished RPM population (Figure 6B). To determine the relative importance of resident RPMs in maintaining the splenic RPM population following transfusions of old RBCs, we used *CCR2*$^{-/-}$ mice, which have Ly6C^{hi} monocytes that do not express CCR2. As a result, Ly6C^{hi} monocytes in *CCR2*$^{-/-}$ mice are confined to the bone marrow and cannot migrate to the spleen in response to CCL2 and/or CCL7[38]; thus, they would be unable to supplement the RPM population that had been depleted by erythrophagocytosis (Figure 6C-D). Using this model, splenic resident RPMs in *CCR2*$^{-/-}$ mice proliferated following the cell death induced by old RBC transfusions, thereby regenerating themselves back to steady-state levels without requiring supplementation by circulating Ly6C^{hi} monocytes (Figure 6E-F).

Macrophages undergo ferroptosis following enhanced erythrophagocytosis

Ferroptosis, in addition to being characterized by increases in ROS production, lipid peroxidation, and *PTGS2* mRNA accumulation, can be rescued by Fer-1, a ferroptosis-specific inhibitor.[11,39] As Fer-1 is not stable in mouse plasma, it is exceedingly difficult to use in vivo. Therefore, we used a cell culture model of enhanced erythrophagocytosis involving exposure of macrophages to IgG antibody-coated RBCs, which markedly increases erythrophagocytosis in vitro in comparison with using old RBCs.[40] By this approach, J774 murine macrophages and primary BMDMs, the latter of which were differentiated for at least 7 days to establish a VCAM-1^{+}, F4/80^{hi} cell population (Figure 7A-C), demonstrated substantial erythrophagocytosis (Figure 7D-E). Following this increased erythrophagocytosis, J774 cells exhibited increased ROS and lipid peroxidation, which were reduced by prior treatment with Fer-1 (Figure 7F-G). Fer-1 induced similar decreases in ROS and lipid peroxidation in BMDMs (Figure 7H-I). Furthermore, BMDMs and J774 cells were sensitive to erastin, RSL3, and imidazole ketone erastin (IKE), which induce ferroptosis in other cell lines (Figure 7J-K),[11,41] indicating their susceptibility to ferroptosis. Finally, we used a high-throughput viability assay with BMDMs that were treated with vehicle control or Fer-1 before ingesting RBCs. By 6 hours after incubation with IgG-opsonized RBCs, BMDMs receiving vehicle control demonstrated substantial cell death, which was effectively prevented by Fer-1 (25.0%-12.0%; Figure 7L). Taken together, these results indicate that ferroptosis plays a major role in erythrophagocytosis-mediated cell death.

Discussion

In our mouse model, RPMs were the predominant splenic population responsible for ingesting old, transfused RBCs (Figure 1A-B). Following this enhanced erythrophagocytosis, RPM cell numbers dramatically declined (Figure 5A), accompanied by increases in ROS, lipid peroxidation, and *PTGS2* gene expression in these cells (Figure 5F-H). Our data in vitro and in vivo strongly suggest that this decline in RPM cell numbers was due to ferroptosis (Figures 5A,F-H and 7F-L), following the substantial increase in erythrophagocytosis experienced by these cells (Figures 1A-B and 7F-I,L). Old RBC transfusions also induced increased *CCL2* and *CCL7* mRNA expression by splenic Ly6C^{hi} monocytes (Figure 4B); this was accompanied by emigration of inflammatory monocytes from the bone marrow into the circulation and then homing to the spleen (Figures 3A-D and 6A), likely a chemotactic response to increased splenic expression of these chemokines. Increased *CCL2* and *CCL7* mRNA expression by splenic Ly6C^{hi} monocytes required the presence of RPMs (Figure 4K), likely due to their clearance of old RBCs and subsequent, as-yet-unidentified, downstream effects. One possibility is that dying RPMs could release heme, which then would stimulate monocyte CCL2 and CCL7 expression by signaling through Toll-like receptor 4.[42] Repopulating the spleen with RPMs following erythrophagocytosis-induced cell death resulted from both local cell division of resident RPMs (Figure 6B) and differentiation of newly arrived circulating Ly6C^{hi} monocytes into RPMs (Figure 6A). Although this highlights a coordinated effort among different cell types to replenish this depleted splenic cell population, RPMs in CCR2-deficient mice were, nonetheless, fully able to repopulate the spleen without requiring an influx of circulating Ly6C^{hi} monocytes (Figure 6E-F). Taken together, this suggests that mice have redundant pathways to maintain, or return to, homeostasis in this setting. Indeed, although both RPM cell division and monocyte migration occur after erythrophagocytosis-mediated RPM ferroptosis, these responses are most likely independent of each other. Thus, monocyte migration from the bone marrow is facilitated by chemokines released from splenic Ly6C^{hi} monocytes as part of an inflammatory response; in contrast, local cell division by remaining RPMs is a macrophage-specific response. Both are likely capable of repopulating the spleen individually, which may be important from an evolutionary perspective.

Ferroptosis is an iron-dependent form of nonapoptotic cell death.[11] Several compounds induce ferroptosis, including erastin,[11] IKE, RSL3,[43] and buthionine sulfoximine.[12] One limitation of Fer-1, a specific inhibitor of ferroptosis, is that it is not stable in mouse plasma, restricting our rescue experiments using this compound to an in vitro model. Ferroptosis is characterized by the accumulation of lipid peroxidation products and lethal ROS derived from iron-dependent reactions. To date, ferroptosis has been described in cancer cells,[11] kidney tubule cells,[39,44,45]

Figure 7 (continued) 100 μM Fer-1 and exposed to IgG-opsonized RBCs; they were then analyzed for ROS (F,H) and lipid peroxidation (G,I). Twenty-four-hour exposure to erastin (20 μM), RSL3 (1 μM), and IKE (20 μM), which are potent ferroptosis inducers, induced BMDM (J) and J774 cell loss (K). BMDM cell viability was quantified following incubation with IgG-opsonized RBCs or PBS, and with vehicle control or 100 μM Fer-1 for 6 hours; enhanced erythrophagocytosis induced substantial cell death, which was ameliorated by Fer-1 (L). Data are representative of 3 independent experiments. *$P < .05$; ***$P < .001$; ****$P < .0001$; ANOVA with the Dunnett multiple comparisons test.

fibroblasts,[44,46] neurons,[47] and T cells,[48] but its occurrence in macrophages is not well studied. As macrophages play important physiological roles in iron metabolism and recycling, the occurrence of ferroptosis (ie, iron-dependent cell death) in these cells is especially relevant. Normal physiological RBCs and iron recycling, where each macrophage clears, on average, 1 RBC per day, does not appear to have any adverse effects on macrophage function. In addition, in response to some degree of enhanced erythrophagocytosis, macrophages can respond homeostatically by increasing their expression of, for example, HO-1 and ferritin, which allow the cell to handle the increased heme and iron load, while still protecting it from severe oxidative stress.[49] As might be expected, there is an increase in *Hmox-1* expression, the mRNA encoding HO-1, soon after transfusion of old RBCs (Figure 1D). However, it is likely, given the number of RBCs that are rapidly ingested, and the accompanying amount of heme iron that needs to be rapidly metabolized and detoxified, that the rate and amount of this increase in *Hmox-1* production is insufficient to prevent cell death. Thus, we believe that the erythrophagocytosis-mediated ferroptotic cell death occurred too rapidly for appropriate increases in *Hmox-1* gene expression, and subsequent HO-1 enzyme synthesis, to occur to prevent catastrophic cell damage. Therefore, our results suggest that substantial erythrophagocytosis can exceed these homeostatic mechanisms, thereby inducing cell death. Furthermore, we would expect worse clinical outcomes in mouse models using exchange transfusions with storage-damaged RBCs (eg, as in hemorrhage-resuscitation models), as compared with the "top-load" transfusions used in our extensively evaluated model,[5,13] which could complicate and confound the outcomes observed.

Given the importance of phagocytes in host defense, including innate, adaptive, and nutritional immunity, it will be important for future studies to determine whether the dramatic, acute, ferroptosis-induced decreases in RPM cell numbers interfere with critical splenic functions, such as clearing circulating pathogenic bacteria during infection and asymptomatic bacteremia. Because an increased incidence of infection following transfusions can exemplify TRIM,[50] whether the effects on RPM cell number seen here represent at least 1 mechanism underlying TRIM is legitimate to question. In addition, given the increased prevalence of dangerous bacterial infections in humans with hemolytic disorders, such as in sickle cell disease[51] and malaria,[52] it will also be important to determine whether immune dysfunction due to erythrophagocytosis-induced phagocyte ferroptosis contributes to these outcomes. Finally, if splenic RPM ferroptosis occurs in other clinically relevant settings exhibiting acute, dramatic increases in erythrophagocytosis, such as IgG-mediated hemolytic transfusion reactions,[2] warm-type autoimmune hemolytic anemia,[3] and acute hemolytic crises in glucose-6-phosphate dehydrogenase deficiency,[4] it could significantly enhance our mechanistic understanding of these disorders and suggest novel therapeutic interventions.

Acknowledgments

The authors thank the Institute of Comparative Medicine for animal housing services. The authors also thank Boguslaw Wojczyk for help in the initial stages of developing the in vitro erythrophagocytosis assay.

L.A.Y. was supported by National Institutes of Health, National Institute of Allergy and Infectious Diseases grant T32 AI106711 and National Institutes of Health, National Heart, Lung, and Blood Institute fellowship F31 HL134284. S.L.S. was supported by National Institutes of Health, National Heart, Lung, and Blood Institute grants R01 HL115557 and R01 HL133049. E.A.H. was supported by National Institutes of Health, National Heart, Lung, and Blood Institute grants R01 HL133049 and R01 HL121275. Research reported in this article was performed in the Columbia Center for Translational Immunology Flow Cytometry Core, supported in part by the Office of the Director, National Institutes of Health under the awards S10RR027050 and S10OD020056.

Authorship

Contribution: L.A.Y. performed and analyzed all experiments, but was assisted by various coauthors; A.R. aided with all mouse experiments; S.P. helped with the high-throughput in vitro viability assay; S.P.W. helped with some flow cytometric data analysis; B.R.S. provided reagents, including IKE and RSL3, and consulted on the experiments characterizing ferroptosis; E.A.H. consulted on the project; S.L.S. provided guidance and aided with analysis and data interpretation; and all authors read and edited the final manuscript.

Conflict-of-interest disclosure: The authors declare no competing financial interests.

ORCID profiles: L.A.Y., 0000-0002-0661-4359; S.L.S., 0000-0002-8528-4561.

Correspondence: Steven L. Spitalnik, Department of Pathology and Cell Biology, Columbia University, 630 W. 168th St, Room P&S 14-434, New York, NY 10032; e-mail: ss2479@cumc.columbia.edu.

Footnotes

Submitted 18 December 2017; accepted 3 April 2018. Prepublished online as *Blood* First Edition paper, 17 April 2018; DOI 10.1182/blood-2017-12-822619.

The publication costs of this article were defrayed in part by page charge payment. Therefore, and solely to indicate this fact, this article is hereby marked "advertisement" in accordance with 18 USC section 1734.

REFERENCES

1. Smith LP, Hunter KW, Oldfield EC, Strickland GT. Murine malaria: blood clearance and organ sequestration of Plasmodium yoelii-infected erythrocytes. *Infect Immun*. 1982;38(1):162-167.

2. Strobel E. Hemolytic transfusion reactions. *Transfus Med Hemother*. 2008;35(5):346-353.

3. Chaudhary RK, Das SS. Autoimmune hemolytic anemia: from lab to bedside. *Asian J Transfus Sci*. 2014;8(1):5-12.

4. Luzzatto L, Nannelli C, Notaro R. Glucose-6-phosphate dehydrogenase deficiency. *Hematol Oncol Clin North Am*. 2016;30(2):373-393.

5. Hod EA, Zhang N, Sokol SA, et al. Transfusion of red blood cells after prolonged storage produces harmful effects that are mediated by iron and inflammation. *Blood*. 2010;115(21):4284-4292.

6. Dixon SJ, Stockwell BR. The role of iron and reactive oxygen species in cell death. *Nat Chem Biol*. 2014;10(1):9-17.

7. Gozzelino R, Soares MP. Coupling heme and iron metabolism via ferritin H chain. *Antioxid Redox Signal*. 2014;20(11):1754-1769.

8. Harrison PM, Arosio P. The ferritins: molecular properties, iron storage function and cellular regulation. *Biochim Biophys Acta*. 1996;1275(3):161-203.

9. Kovtunovych G, Eckhaus MA, Ghosh MC, Ollivierre-Wilson H, Rouault TA. Dysfunction of the heme recycling system in heme oxygenase 1-deficient mice: effects on macrophage viability and tissue iron distribution. *Blood*. 2010;116(26):6054-6062.

10. Theurl I, Hilgendorf I, Nairz M, et al. On-demand erythrocyte disposal and iron recycling requires transient macrophages in the liver. *Nat Med*. 2016;22(8):945-951.

11. Dixon SJ, Lemberg KM, Lamprecht MR, et al. Ferroptosis: an iron-dependent form of non-apoptotic cell death. *Cell*. 2012;149(5):1060-1072.

12. Yang WS, SriRamaratnam R, Welsch ME, et al. Regulation of ferroptotic cancer cell death by GPX4. *Cell*. 2014;156(1-2):317-331.

13. Gilson CR, Kraus TS, Hod EA, et al. A novel mouse model of red blood cell storage and posttransfusion in vivo survival. *Transfusion*. 2009;49(8):1546-1553.

14. US Department of Health and Human Services. The 2011 National Blood Collection and Utilization Survey Report. Washington, DC: Office of the Assistant Secretary for Health, US Department of Health and Human Services; 2013.

15. Carson JL, Brooks MM, Abbott JD, et al. Liberal versus restrictive transfusion thresholds for patients with symptomatic coronary artery disease. *Am Heart J*. 2013;165(6):964-971.e1.

16. Rohde JM, Dimcheff DE, Blumberg N, et al. Health care-associated infection after red blood cell transfusion: a systematic review and meta-analysis. *JAMA*. 2014;311(13):1317-1326.

17. Purdy FR, Tweeddale MG, Merrick PM. Association of mortality with age of blood transfused in septic ICU patients. *Can J Anaesth*. 1997;44(12):1256-1261.

18. Zallen G, Offner PJ, Moore EE, et al. Age of transfused blood is an independent risk factor for postinjury multiple organ failure. *Am J Surg*. 1999;178(6):570-572.

19. Tinmouth A, Fergusson D, Yee IC, Hébert PCABLE Investigators; Canadian Critical Care Trials Group. Clinical consequences of red cell storage in the critically ill. *Transfusion*. 2006;46(11):2014-2027.

20. Vandromme MJ, McGwin G Jr, Marques MB, Kerby JD, Rue LW III, Weinberg JA. Transfusion and pneumonia in the trauma intensive care unit: an examination of the temporal relationship. *J Trauma*. 2009;67(1):97-101.

21. Offner PJ, Moore EE, Biffl WL, Johnson JL, Silliman CC. Increased rate of infection associated with transfusion of old blood after severe injury. *Arch Surg*. 2002;137(6):711-717.

22. Callan MB, Patel RT, Rux AH, et al. Transfusion of 28-day-old leucoreduced or non-leucoreduced stored red blood cells induces an inflammatory response in healthy dogs. *Vox Sang*. 2013;105(4):319-327.

23. Kim-Shapiro DB, Lee J, Gladwin MT. Storage lesion: role of red blood cell breakdown. *Transfusion*. 2011;51(4):844-851.

24. Haradin AR, Weed RI, Reed CF. Changes in physical properties of stored erythrocytes relationship to survival in vivo. *Transfusion*. 1969;9(5):229-237.

25. Berezina TL, Zaets SB, Morgan C, et al. Influence of storage on red blood cell rheological properties. *J Surg Res*. 2002;102(1):6-12.

26. Hess JR. Red cell changes during storage. *Transfus Apheresis Sci*. 2010;43(1):51-59.

27. Kalyanaraman B, Darley-Usmar V, Davies KJA, et al. Measuring reactive oxygen and nitrogen species with fluorescent probes: challenges and limitations. *Free Radic Biol Med*. 2012;52(1):1-6.

28. Haldar M, Kohyama M, So AY-L, et al. Heme-mediated SPI-C induction promotes monocyte differentiation into iron-recycling macrophages. *Cell*. 2014;156(6):1223-1234.

29. Meinderts SM, Oldenborg PA, Beuger BM, et al. Human and murine splenic neutrophils are potent phagocytes of IgG-opsonized red blood cells. *Blood Adv*. 2017;1(14):875-886.

30. Shi C, Pamer EG. Monocyte recruitment during infection and inflammation. *Nat Rev Immunol*. 2011;11(11):762-774.

31. Tsou C-L, Peters W, Si Y, et al. Critical roles for CCR2 and MCP-3 in monocyte mobilization from bone marrow and recruitment to inflammatory sites. *J Clin Invest*. 2007;117(4):902-909.

32. Jia T, Serbina NV, Brandl K, et al. Additive roles for MCP-1 and MCP-3 in CCR2-mediated recruitment of inflammatory monocytes during Listeria monocytogenes infection. *J Immunol*. 2008;180(10):6846-6853.

33. Kohyama M, Ise W, Edelson BT, et al. Role for Spi-C in the development of red pulp macrophages and splenic iron homeostasis. *Nature*. 2009;457(7227):318-321.

34. Burnett SH, Kershen EJ, Zhang J, et al. Conditional macrophage ablation in transgenic mice expressing a Fas-based suicide gene. *J Leukoc Biol*. 2004;75(4):612-623.

35. Xie Y, Hou W, Song X, et al. Ferroptosis: process and function. *Cell Death Differ*. 2016;23(3):369-379.

36. Hashimoto D, Chow A, Noizat C, et al. Tissue-resident macrophages self-maintain locally throughout adult life with minimal contribution from circulating monocytes. *Immunity*. 2013;38(4):792-804.

37. Schulz C, Perdiguero EG, Chorro L, et al. A lineage of myeloid cells independent of Myb and hematopoietic stem cells. *Science*. 2012;336(6077):86-90.

38. Boring L, Gosling J, Chensue SW, et al. Impaired monocyte migration and reduced type 1 (Th1) cytokine responses in C-C chemokine receptor 2 knockout mice. *J Clin Invest*. 1997;100(10):2552-2561.

39. Linkermann A, Skouta R, Himmerkus N, et al. Synchronized renal tubular cell death involves ferroptosis. *Proc Natl Acad Sci USA*. 2014;111(47):16836-16841.

40. Wojczyk BS, Kim N, Bandyopadhyay S, et al. Macrophages clear refrigerator storage-damaged red blood cells and subsequently secrete cytokines in vivo, but not in vitro, in a murine model. *Transfusion*. 2014;54(12):3186-3197.

41. Larraufie M-H, Yang WS, Jiang E, Thomas AG, Slusher BS, Stockwell BR. Incorporation of metabolically stable ketones into a small molecule probe to increase potency and water solubility. *Bioorg Med Chem Lett*. 2015;25(21):4787-4792.

42. Fortes GB, Alves LS, de Oliveira R, et al. Heme induces programmed necrosis on macrophages through autocrine TNF and ROS production. *Blood*. 2012;119(10):2368-2375.

43. Yang WS, Stockwell BR. Synthetic lethal screening identifies compounds activating iron-dependent, nonapoptotic cell death in oncogenic-RAS-harboring cancer cells. *Chem Biol*. 2008;15(3):234-245.

44. Friedmann Angeli JP, Schneider M, Proneth B, et al. Inactivation of the ferroptosis regulator Gpx4 triggers acute renal failure in mice. *Nat Cell Biol*. 2014;16(12):1180-1191.

45. Skouta R, Dixon SJ, Wang J, et al. Ferrostatins inhibit oxidative lipid damage and cell death in diverse disease models. *J Am Chem Soc*. 2014;136(12):4551-4556.

46. Gao M, Monian P, Quadri N, Ramasamy R, Jiang X. Glutaminolysis and transferrin regulate ferroptosis. *Mol Cell*. 2015;59(2):298-308.

47. Chen L, Hambright WS, Na R, Ran Q. Ablation of the ferroptosis inhibitor glutathione peroxidase 4 in neurons results in rapid motor neuron degeneration and paralysis. *J Biol Chem*. 2015;290(47):28097-28106.

48. Matsushita M, Freigang S, Schneider C, Conrad M, Bornkamm GW, Kopf M. T cell lipid peroxidation induces ferroptosis and prevents immunity to infection. *J Exp Med*. 2015;212(4):555-568.

49. Soares MP, Hamza I. Macrophages and iron metabolism. *Immunity*. 2016;44(3):492-504.

50. Youssef LA, Spitalnik SL. Transfusion-related immunomodulation: a reappraisal. *Curr Opin Hematol*. 2017;24(6):551-557.

51. Johnston RB Jr, Newman SL, Struth AG. Increased susceptibility to infection in sickle cell disease: defects of opsonization and of splenic function. *Birth Defects Orig Artic Ser*. 1975;11(1):322-327.

52. Cunnington AJ, de Souza JB, Walther M, Riley EM. Malaria impairs resistance to Salmonella through heme- and heme oxygenase-dependent dysfunctional granulocyte mobilization. *Nat Med*. 2011;18(1):120-127.